Analysis of a new hybrid method for immiscible two-phase multicomponent flow through porous media

Prabir Daripa* and Sourav Dutta†
Department of Mathematics, Texas A&M University
College Station, TX 77843-3368

October 26, 2016

Abstract

A convergence study is performed for a new hybrid method of solving the system of equations that govern the multicomponent flow of two incompressible, immiscible fluid phases through porous media. The theoretical convergence results are supported by numerical simulations of a polymer flood in a quarter five-spot geometry. The numerical results obtained with the finest spatial grid are compared with results on a sequence of coarser spatial grids.

Keywords— multicomponent two-phase flow, capillary pressure, finite element method, method of characteristics, convergence analysis, numerical simulations

1 Introduction

In this paper, we outline a model that describes the incompressible, multicomponent, immiscible flow of two fluid phases through porous media and discuss a hybrid numerical method to solve the model. The model problem that we use as an example of a multicomponent, immiscible, two-phase porous media flow is a chemical Enhanced Oil Recovery (EOR) method called Polymer flooding, in which a polymer laden aqueous phase is injected into the porous oil reservoirs. Polymer enhances oil recovery by improving the mobility ratio between the displaced phase (oil) and the displacing phase (aqueous). We consider the system of partial differential equations governing the flow written in terms of the global pressure (see [1]), which gives rise to a system of coupled elliptic-parabolic equations. The numerical method uses a combination of a non-traditional discontinuous finite element method and a time implicit finite difference method based on the Modified Method Of Characteristics (MMOC). We present a detailed convergence analysis of the method. For the purpose of validating the numerical method we restrict ourselves to the numerical simulation of quarter five-spot flooding in horizontal, two dimensional reservoirs.

Classical finite difference [2, 3] and finite element methods often give rise to nonphysical oscillations in the numerical solution while classical upwind methods tend to generate excessive numerical diffusion that smears out the fronts and can also cause other spurious effects due to grid orientation problems [4, 5]. The locally mass conservation property of *finite volume methods* [6, 7] provides an added advantage for the numerical simulation of oil reservoirs. Some popular *finite element* based methods such as control volume (CVFE), discontinuous (DG -[8, 9]) and mixed FE [10] do not suffer from much grid orientation effects, allow local grid refinement and have high order of accuracy.

An alternative approach to solve time dependent advection-diffusion problems is given by the class of Eulerian-Lagrangian methods. Such methods combine the advection and capacity terms in the transport

*Author for correspondence (email:daripa@math.tamu.edu)
†email:sdutta@math.tamu.edu

equations to execute the temporal discretization in the Lagrangian coordinates while a fixed mesh in the Eulerian coordinates is employed for the diffusion term [11, 12]. These methods not only stabilize the numerical approximations to improve accuracy but also significantly reduce the numerical diffusion and grid-orientation effects observed in upwind schemes, and are very competitive in terms of accuracy and efficiency [13, 14]. The modified method of characteristics (MMOC) is one of the earliest methods [15] in the class of Eulerian-Lagrangian methods to be widely accepted for numerical simulation of miscible and immiscible displacement problems [4]. Some of the significant subsequent improvements on this method include the modified method of characteristics with adjusted advection (MMOCAA) [16], the Eulerian-Lagrangian localized adjoint method (ELLAM) [17], the characteristic mixed finite element method (CMFEM) [18], the characteristic finite volume element method (CFVEM) [19] and the Eulerian-Lagrangian discontinuous Galerkin method (ELDG) [20]. The MMOCAA is a mass-conserving time discretization procedure which inherits the competitiveness of the MMOC. The conservative modified method of characteristics (CMMOC)[21] is a variant of the MMOCAA which adjusts the convection implicitly and minimizes the error of the mass balance problem. The ELLAM and CMFEM are some of the other variants of the characteristics based method which also conserve mass.

Error estimates and convergence analysis have been carried out extensively for the MMOC [15], the MMOCAA [22], the CMFEM [18], the ELLAM [23, 12] and the ELDG [20] methods. In most of these estimates the generic constants are inversely dependent on the vanishing parameter ϵ and cause difficulties when ϵ approaches 0. The uniformly optimal-order convergence rates that are observed numerically for Eulerian-Lagrangian methods are often not reflected in these estimates. Some, ϵ-uniform estimates for the advection diffusion equations with diffusion of the form $\epsilon D(x,t)$ and with periodic and flux boundary conditions were obtained for the MMOC, the MMOCAA, the ELLAM and the ELDG schemes (see [20] and references therein). Although all of these estimates are ϵ-independent, they depend strongly on the lower and the upper bounds of the diffusion coefficient $D(x,t)$.

In this paper, we consider the model and the hybrid method for multicomponent, immiscible two-phase flow in porous media, proposed in [1], which describes the displacement processes in terms of a new global pressure formulation and uses a combination of a non-traditional discontinuous finite element method with a MMOC based implicit time finite difference scheme for solving the advection-diffusion equations. In [1], the method was validated numerically by comparing with an exact two dimensional solution of two-phase flow. In this paper, we present the convergence analysis of the method. We support the theoretical results by computing L^2 and L^∞ error norms for numerical solutions of two dimensional polymer flooding, obtained by uniform spatial grid and time step refinement. The rest of the paper is laid out as follows. In section 2, the governing equations for incompressible, multicomponent, immiscible two-phase flow of fluids through porous media are presented with the global pressure, the wetting phase saturation and the component concentration as the primary variables. In section 3, we present the numerical method: the computational grids, the non-traditional discontinuous finite element method, the MMOC based finite difference scheme for the transport equations and the computational algorithm. In section 4, we discuss the convergence characteristics of the method. We present and discuss the numerical results in section 5. Finally section 6 contains concluding remarks.

2 Model problem

Let Ω be a finite domain in $\mathbb{R}^2$ representing the porous medium with boundary $\partial\Omega$. The incompressible and immiscible flow of the wetting phase (water or an aqueous solution of polymer and/or surfactant) and the non-wetting phase (oil) in Ω over a time interval $[0,T]$ is described by a combination of the multiphase extension of Darcy's law (see [24]) for each phase and transport equations for each species. Let s_j denote the saturation (volume fraction), $\mathbf{v}_j$ denote the velocity, p_j denote the phase pressure and q_j denote the volumetric injection/production rate of phase j where $j = o$ or $j = a$ denotes the non-wetting and wetting phase respectively. Then considering the hypothesis of capillary pressure and using the conservation of mass principle, we write the transport equation satisfied by each phase saturation, s_j as

$$\phi \frac{\partial s_j}{\partial t} + \boldsymbol{\nabla} \cdot \mathbf{v}_j = q_j, \quad (\mathbf{x}, t) \in \Omega \times (0, T], \quad j = a,\, o. \tag{1}$$

The conservation of mass of any species dissolved in the aqueous phase gives rise to:

$$\phi \frac{\partial (c s_a)}{\partial t} + \nabla \cdot (c \mathbf{v}_a) = c_{inj} q_a, \quad (\mathbf{x}, t) \in \Omega \times (0, T], \tag{2}$$

where c is the concentration (volume fraction in the aqueous phase) of the dissolved species, c_{inj} is the concentration of the species in the injected fluid and the inherent assumption is that the species is getting only passively advected with negligible diffusion. Using conservation of momentum of each phase, the phase velocity v_j is found to obey the extended Darcy's law:

$$\mathbf{v}_j = -\mathbf{K}(\mathbf{x}) \lambda_j \boldsymbol{\nabla} p_j, \quad \mathbf{x} \in \Omega, \quad j = a,\, o. \tag{3}$$

Here ϕ is the porosity (taken to be constant in this study), $\mathbf{K}(\mathbf{x})$ is the absolute permeability tensor of the porous medium, $\lambda = \lambda_a(s, c) + \lambda_o(s, c)$ is the total mobility and $\lambda_j = k_{rj}/\mu_j$ is the phase mobility where k_{rj} is the relative permeability and μ_j is the viscosity of phase j. In addition to the above, we impose the capillary pressure (p_c) equation for the immiscible phases:

$$p_c = p_o - p_a. \tag{4}$$

We also consider the porous medium to be initially saturated with the two phases and hence we get the equation:

$$\sum_{j=o,a} s_j = 1. \tag{5}$$

The combination of the above equations produces a system of strongly coupled nonlinear equations which suffer from potential degeneracy. In order to avoid this difficulty we reformulate the problem by using the global pressure (p) for incompressible, immiscible two-phase flows with dissolved components (see [1]) defined by:

$$\begin{aligned} p = \frac{1}{2}(p_o + p_a) &+ \frac{1}{2} \int_{s_c}^{s} \left(\hat{\lambda}_o(\zeta, c) - \hat{\lambda}_a(\zeta, c) \right) \frac{dp_c}{d\zeta}(\zeta) d\zeta \\ &- \frac{1}{2} \int \left(\int_{s_c}^{s} \frac{\partial}{\partial c} \left(\hat{\lambda}_o(\zeta, c) - \hat{\lambda}_a(\zeta, c) \right) \frac{dp_c}{d\zeta}(\zeta) d\zeta \right) \left(\frac{\partial c}{\partial x} dx + \frac{\partial c}{\partial y} dy \right) \end{aligned} \tag{6}$$

where $\hat{\lambda}_j = \lambda_j / \lambda$ for $j = a, o$ and s_c is the value of the aqueous phase saturation at which $p_c(s_c) = 0$. The global pressure is well defined for all values of s_a in $[1 - s_{ro}, s_{ra}]$ where s_{ra} (resp. s_{ro}) is the residual saturation of the wetting phase (resp. non-wetting phase). If we write $s_a = s$, an equivalent formulation of the problem is obtained in terms of the primary variables (p, s, c) :

$$-\boldsymbol{\nabla} \cdot (\mathbf{K}(\mathbf{x}) \lambda \boldsymbol{\nabla} p) = \tilde{q} \equiv \Sigma_i \tilde{q}^{(i)} \delta(\mathbf{x} - \mathbf{x}^{(i)}), \qquad \mathbf{x} \in \Omega,\ t \in (0, T] \tag{7a}$$

$$\phi s_t + \boldsymbol{\nabla} \cdot (-\mathbf{K}(\mathbf{x}) \lambda f \boldsymbol{\nabla} p + \boldsymbol{D} \boldsymbol{\nabla} p_c) = q_a, \qquad \mathbf{x} \in \Omega,\ t \in (0, T] \tag{7b}$$

$$\phi (sc)_t + \boldsymbol{\nabla} \cdot (-\mathbf{K}(\mathbf{x}) \lambda c f \boldsymbol{\nabla} p + \boldsymbol{D} \boldsymbol{\nabla} p_c) = c_{inj} q_a, \qquad \mathbf{x} \in \Omega,\ t \in (0, T] \tag{7c}$$

where $\boldsymbol{D} = \mathbf{K}(\mathbf{x}) \lambda_o f$ and $\tilde{q} = q_o + q_a$ is an appropriate source term for the pressure equation which denotes net volume of fluid, the non-wetting phase (q_o) and the wetting phase (q_a), injected per unit volume per unit time. For numerical purposes, this is modeled by a finite number of point sources and sinks located at isolated points $\mathbf{x}^{(i)}$ so that $\tilde{q} = \Sigma_i \tilde{q}^{(i)} \delta(\mathbf{x} - \mathbf{x}^{(i)})$. The following initial and boundary conditions are prescribed:

$$\forall \mathbf{x} \in \Omega: \qquad s(\mathbf{x}, 0) = s_0(\mathbf{x}) \quad \& \quad c(\mathbf{x}, 0) = c_0(\mathbf{x}), \tag{8a}$$

$$\forall (\mathbf{x}, t) \in \partial\Omega \times (0, T]: \quad \frac{\partial s}{\partial n} = 0, \quad \frac{\partial c}{\partial n} = 0 \quad \& \quad \mathbf{v}_j \cdot \hat{n} = 0, \, (j = a, o) \tag{8b}$$

where $\hat{n}$ denotes the outward unit normal to $\partial\Omega$. We also make some practical and physical assumptions:

$$q_a = \tilde{q} \quad \text{and} \quad q_o = 0 \quad \text{when } \tilde{q} \geq 0, \tag{9}$$

$$q_a = \lambda_a \tilde{q} \quad \text{and} \quad q_o = \lambda_o \tilde{q} \quad \text{when } \tilde{q} < 0, \tag{10}$$

which mean that oil is never injected and the fluid mixture obtained at the production well is proportional to the resident fluid at the point. Several models of relative permeability, k_{rj} and capillary pressure are available in the literature (see [25, 26, 27]). In this study, we use the following Van Genuchten model ([28]) which assumes that the residual wetting phase and non-wetting phase saturation are zero.

$$k_{ra}(s) = s^{1/2} \left(1 - (1 - s^{1/m})^m\right)^2, \tag{11a}$$

$$k_{ro}(s) = s^{1/2} \left(1 - (1 - s^{1/m})^m\right)^{2m}, \tag{11b}$$

$$p_c(s) = \frac{1}{\alpha_0} \left(s^{-1/m} - 1\right)^{1-m}. \tag{11c}$$

The values of the parameters m and α_0 in the above model are known to depend on the interfacial tension, $\sigma 0$ between the non-wetting and the wetting phases. In our study below we take $m = 2/3$ and $\alpha_0 = 0.125$ (see [29]). Alternatively Corey-type imbibition relations can also be used (see [25] and [26]). These models assume that p_c and $k_{rj} (j = a, o)$ are nonlinear functions of only the wetting phase saturation, s, which is a valid assumption for polymer flooding. In Surfactant-Polymer (SP) flooding, a small amount of a suitable surfactant is added to the polymer laden aqueous solution, as surfactant further improves oil recovery by reducing the capillary pressure between the aqueous and the oil phases and also by reducing the residual saturation limits of the rock matrix. Therefore, during SP flooding p_c and $k_{rj} (j = a, o)$ are known to depend on both s and the concentration, Γ of the surfactant. For a detailed discussion on the models needed for such a study see [1]. For the purpose of a convergence study, here we restrict ourselves to the simpler case of polymer flooding.

3 Numerical scheme

The system of coupled transport equations given by eqs. (7b) and (7c) is solved using a combination of the MMOC and an implicit time finite difference scheme. For the computational grid, we partition the domain Ω into rectangular cells. Given positive integers $I, J \in \mathcal{Z}^+$, set $\Delta x = (x_{max} - x_{min})/I = 1/I$ and $\Delta y = (y_{max} - y_{min})/J = 1/J$. We define a uniform Cartesian grid $(x_i, y_j) = (i\Delta x, j\Delta y)$ for $i = 0, ..., I$ and $j = 0, ..., J$. Each (x_i, y_j) is called a grid point. For the case $i = 0, I$ or $j = 0, J$, a grid point is called a boundary point, otherwise it is called an interior point. In general, the grid size is defined as $h = max(\Delta x, \Delta y) > 0$. However, in this paper we use an uniform spatial grid: $\Delta x = \Delta y = h$.

The elliptic flow equation eq. (7a) for global pressure is solved using a discontinuous finite element method on a non-body-fitted grid which is constructed in the following way. We introduce uniform triangulations inside the grid generated for the transport equations eqs. (7b) and (7c). This means every rectangular region $[x_i, x_{i+1}] \times [y_j, y_{j+1}]$ is cut into two pieces of right triangular regions: one is bounded by $x = x_i, y = y_j$ and $y = \frac{y_{j+1} - y_j}{x_i - x_{i+1}}(x - x_{i+1}) + y_j$, the other is bounded by $x = x_{i+1}, y = y_{j+1}$ and $y = \frac{y_{j+1} - y_j}{x_i - x_{i+1}}(x - x_{i+1}) + y_j$. Collecting all those triangular regions, also called elements, we obtain a uniform triangulation, $L^h = \{\kappa | \kappa \text{ is a triangular element}\}$. We may also choose the hypotenuse to be $y = \frac{y_{j+1} - y_j}{x_{i+1} - x_i}(x - x_i) + y_j$, and get another uniform triangulation from the same Cartesian grid. There is no conceptual difference on these two triangulations for our method.

3.1 Flow equation

The elliptic equation describing the evolution of global pressure is:

$$-\boldsymbol{\nabla}\cdot(\mathbf{K}(\mathbf{x})\lambda\boldsymbol{\nabla}p)=\tilde{q},\qquad \mathbf{x}\in\Omega\backslash\Sigma, \tag{12a}$$

$$(\mathbf{K}(\mathbf{x})\lambda\boldsymbol{\nabla}p)\cdot\hat{\mathbf{n}}=0,\qquad \mathbf{x}\in\partial\Omega, \tag{12b}$$

where Σ denotes the union of the interfaces that separate Ω into several subdomains. However, for simplicity of exposition, here we assume that we have only two separated subdomains, Ω^+ and Ω^-. The following kinematic condition holds at the interface Σ:

$$[\mathbf{K}(\mathbf{x})\lambda\boldsymbol{\nabla}p\cdot\hat{\mathbf{n}}]_\Sigma=0, \tag{13}$$

where $\hat{\mathbf{n}}$ is the outward unit normal which points from Ω^- to Ω^+ and $[\,]$ denotes a jump. We assume the boundary $\partial\Omega$ and the interface Σ to be Lipschitz continuous. Hence a unit normal vector, $\hat{\mathbf{n}}$ can be defined a.e. on Σ. This problem is solved using a non-traditional finite element formulation (see [30]) which is second order accurate in the L^∞ norm for matrix coefficient elliptic equations with discontinuities across the interfaces. The weak formulation of eqs. (12a) and (12b) in the usual Sobolev spaces $H^1(\Omega)$ with $\psi\in H^1(\Omega)$ is given by:

$$\int\limits_{\Omega^+}\mathbf{K}\lambda\boldsymbol{\nabla}p\boldsymbol{\nabla}\psi+\int\limits_{\Omega^-}\mathbf{K}\lambda\boldsymbol{\nabla}p\boldsymbol{\nabla}\psi-\int\limits_{\partial\Omega}\mathbf{K}\lambda\psi\boldsymbol{\nabla}p.\hat{\mathbf{n}}=\int\limits_{\Omega}f\psi \tag{14}$$

where $\mathbf{f}$ denotes the source term, $\tilde{q}$.

The elements, κ of triangulation, L^h, are classified into regular cells and interface cells. We call κ a regular cell if its vertices are in the same subdomain and an interface cell when its vertices belong to different subdomains. For an interface cell, $\kappa=\kappa^+\cup\kappa^-$ where κ^+ and κ^- are separated by a line segment Σ_k^h, obtained by joining the two points where the interface Σ intersects the sides or the vertices of that interface cell. A set of grid functions, $H^{1,h}=\{\omega^h\,|\,\omega^h=\omega_{i,j}\,;\,0\le i\le I, 0\le j\le J\}$ are defined on the grid points of the mesh L^h. An extension operator $U^h: H^{1,h}\to H^1(\kappa)$ is constructed as follows. For any $\phi^h\in H^{1,h}$, $U^h(\phi^h)$ is a piecewise linear function and matches ϕ^h on the grid points. In a regular cell, it is a linear function that interpolates the values of ϕ^h at the grid points. In an interface cell, it consists of two pieces of linear functions, one each defined on κ^+ and κ^-. The location of the discontinuity of the extended function $U^h(\phi^h)$ in an interface cell is on the line segment Σ_k^h. Hence an interface jump condition on the pressure, p, if there is one, can be imposed on the two end points of this line segment at $\{\partial\kappa\}\cap\{\Sigma_k^h\}$ while the interface jump condition, eq. (13), is imposed at the middle point of Σ_k^h. The construction of such extension operators and proof of their uniqueness is found in the literature [30, 31].

Using the extension functions as discussed above (also see [1]), the weak formulation eq. (14) reduces to finding a discrete function $\phi^h\in H^{1,h}$ such that it satisfies Eq. (12b) on the boundary points and so that for all $\psi^h\in H^{1,h}$,

$$\begin{aligned}&\sum_{K\in L^h}\left(\int\limits_{K^+}\mathbf{K}\lambda\;\boldsymbol{\nabla}U^h(\phi^h)\boldsymbol{\nabla}U^h(\psi^h)+\int\limits_{K^-}\mathbf{K}\lambda\;\boldsymbol{\nabla}U^h(\phi^h)\boldsymbol{\nabla}U^h(\psi^h)\right)\\&-\sum_{K\in L^h}\int\limits_{\partial K}\mathbf{K}\lambda\;U^h(\psi^h)\boldsymbol{\nabla}U^h(\phi^h)\cdot\hat{\mathbf{n}}=\sum_{K\in L^h}\left(\int\limits_{K^+}f\,U^h(\psi^h)+\int\limits_{K^-}f\,U^h(\psi^h)\right).\end{aligned} \tag{15}$$

It can be shown that if $\mathbf{K}(\mathbf{x})$ is positive definite, then the matrix obtained for the linear system of the discretized weak form, eq. (15), is also positive definite and is therefore invertible.

3.2 Transport equations

The transport equations, eq. (7b) and eq. (7c), are solved using a Modified version of the Method Of Characteristics (MMOC). At first we rewrite eqs. (7b) and (7c) in a non-conservative form as follows

$$\phi s_t + \frac{\partial f}{\partial s}\mathbf{v}\cdot\boldsymbol{\nabla} s + \boldsymbol{\nabla}\cdot(\boldsymbol{D}\boldsymbol{\nabla} s) = g_1 - \frac{\partial f}{\partial c}\mathbf{v}\cdot\boldsymbol{\nabla} c \tag{16a}$$

$$\phi c_t + \left(\frac{f}{s}\mathbf{v} + \frac{\boldsymbol{D}}{s}\boldsymbol{\nabla} s\right)\cdot\boldsymbol{\nabla} c + c\frac{g_1}{s} = \frac{g_2}{s} \tag{16b}$$

where $\boldsymbol{D}(s,c) = \mathbf{K}(\mathbf{x})\lambda_o(s)f(s,c)\frac{dp_c(s)}{ds}$, $g_1 = q_a$ and $g_2 = c_{inj}q_a$. In eq. (16a) we replace the transport operator, $\phi s_t + \frac{\partial f}{\partial s}\mathbf{v}\cdot\boldsymbol{\nabla} s$ by a derivative along its characteristic direction in the following way

$$\frac{\partial}{\partial \tau_s} = \frac{1}{\psi_s}\left(\phi\frac{\partial}{\partial t} + \frac{\partial f}{\partial s}\mathbf{v}\cdot\boldsymbol{\nabla}\right) \tag{17}$$

where τ_s is used to parametrize the characteristics and ψ_s is a suitable normalization that simplifies the numerical discretization of the characteristic derivative and is defined by

$$\psi_s = \left[\phi^2 + \left(\frac{\partial f}{\partial s}\right)^2 |\mathbf{v}|^2\right]^{1/2} \tag{18}$$

Then eq. (16a) is equivalently written in the form

$$\psi_s\frac{\partial s}{\partial \tau_s} + \boldsymbol{\nabla}\cdot(\boldsymbol{D}\boldsymbol{\nabla} s) = g_1 - \frac{\partial f}{\partial c}\mathbf{v}\cdot\boldsymbol{\nabla} c \tag{19}$$

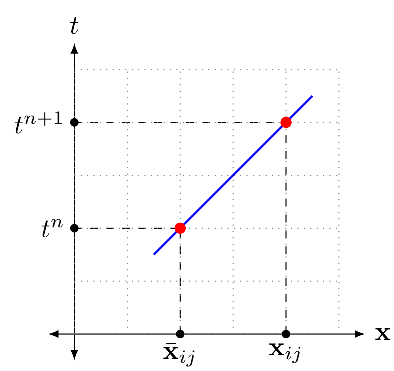

Figure 1: Discrete approximation of the characteristic curve from $\bar{\mathbf{x}}_{ij}$ to $\mathbf{x}_{ij}$ in 1D

For numerical computation, we use the spatial grid described in the beginning of § 3 and the time interval $[0,T]$ is uniformly divided into N subintervals of length Δt, such that $t^n = n\Delta t$ and $T = N\Delta t$. Then we denote the grid values of the variables by $w_{ij}^n = w(\mathbf{x}_{ij}, t^n)$ where $\mathbf{x}_{ij} = \mathbf{x}(ih, jh)$. Consider that the solution is known at some time t^n and the solution at a subsequent time t^{n+1} needs to be computed. Then starting from any point $(\mathbf{x}_{ij}, t^{n+1})$ we trace backward along the characteristics to a point $(\bar{\mathbf{x}}_{ij}, t^n)$ where the solution is already known. As shown in Figure 1, let the characteristics which originate from the point $\bar{\mathbf{x}}_{ij}$ at time t^n reach the point $\mathbf{x}_{ij}$ at time t^{n+1}. From the equation of the characteristic curves given by

$$\frac{d\mathbf{x}}{d\tau_s} = \frac{1}{\phi}\frac{\partial f}{\partial s}\mathbf{v}$$

we use numerical discretization to obtain an approximate value of $\bar{\mathbf{x}}_{ij}$ in the following way

$$\bar{\mathbf{x}}_{ij} = \mathbf{x}_{ij} - \frac{\partial f}{\partial s}(s_{ij}^n, c_{ij}^n)\mathbf{v}_{ij}^n \Delta t/\phi.$$

Using the above equation, the derivative in the characteristic direction, defined by eq. (17), is approximated by:

$$\psi_s \frac{\partial s}{\partial \tau_s} \approx \psi_s \frac{s(\mathbf{x}_{ij}, t^{n+1}) - s(\bar{\mathbf{x}}_{ij}, t^n)}{\left[|\mathbf{x}_{ij} - \bar{\mathbf{x}}_{ij}|^2 + (\Delta t)^2\right]^{1/2}} = \phi \frac{s_{ij}^{n+1} - \bar{s}_{ij}^n}{\Delta t} \quad (\text{ see § 4 })$$

This leads to the following implicit-time finite difference formulation for eq. (19)

$$\phi \frac{s_{ij}^{n+1} - \bar{s}_{ij}^n}{\Delta t} + \boldsymbol{\nabla}_h (\bar{\boldsymbol{D}} \boldsymbol{\nabla}_h s)_{ij}^{n+1} = (g_1)_{ij} - \left(\frac{\partial f}{\partial c}\right)_{ij}^n (\mathbf{v}_{ij}^n \cdot \boldsymbol{\nabla}_h c_{ij}^n) \tag{20}$$

where

$$\begin{aligned}
\bar{s}_{ij}^n &= s(\bar{\mathbf{x}}_{ij}, t^n) \qquad \& \qquad \bar{\boldsymbol{D}}_{ij}^n = \boldsymbol{D}(\bar{s}_{ij}^n, c_{ij}^n) \\
\boldsymbol{\nabla}_h (\bar{\boldsymbol{D}} \nabla_h s)_{ij}^{n+1} &= \bar{\boldsymbol{D}}_{i+1/2,j} \frac{s_{i+1,j}^{n+1} - s_{i,j}^{n+1}}{\Delta x^2} - \bar{\boldsymbol{D}}_{i-1/2,j} \frac{s_{i,j}^{n+1} - s_{i-1,j}^{n+1}}{\Delta x^2} \\
&\quad + \bar{\boldsymbol{D}}_{i,j+1/2} \frac{s_{i,j+1}^{n+1} - s_{i,j}^{n+1}}{\Delta y^2} - \bar{\boldsymbol{D}}_{i,j-1/2} \frac{s_{i,j}^{n+1} - s_{i,j-1}^{n+1}}{\Delta y^2} \\
\bar{\boldsymbol{D}}_{i\pm 1/2,j} &= \frac{\boldsymbol{D}(\bar{s}_{i\pm 1,j}^n, c_{i\pm 1,j}^n) + \boldsymbol{D}(\bar{s}_{i,j}^n, c_{i,j}^n)}{2} \\
\bar{\boldsymbol{D}}_{i,j\pm 1/2} &= \frac{\boldsymbol{D}(\bar{s}_{i,j\pm 1}^n, c_{i,j\pm 1}^n) + \boldsymbol{D}(\bar{s}_{i,j}^n, c_{i,j}^n)}{2}
\end{aligned}$$

Following the same procedure as before we define the following equations, analogous to eqs. (17)–(19), for the concentration equation eq. (16b):

$$\begin{aligned}
\psi_c &= \left[\phi^2 + \left(\frac{f}{s}\right)^2 |\mathbf{v}|^2 + \left(\frac{\boldsymbol{D}}{s}\right)^2 |\nabla s|^2\right]^{1/2} \\
\frac{\partial}{\partial \tau_c} &= \frac{1}{\psi_c}\left(\phi \frac{\partial}{\partial t} + \frac{f}{s}\mathbf{v} \cdot \nabla + \frac{\boldsymbol{D}}{s} \nabla s \cdot \nabla\right)
\end{aligned}$$

Then using the updated saturation values, the derivative in the characteristic direction, τ_c of the operator $\phi c_t + \frac{f}{s}\mathbf{v} \cdot \boldsymbol{\nabla} s + \frac{\boldsymbol{D}}{s} \boldsymbol{\nabla} s \cdot \boldsymbol{\nabla} c$ is approximated using the following:

$$\bar{\mathbf{x}}_{ij}^c = \mathbf{x}_{ij}^c - \left(\left(\frac{f}{s}\right)(s_{ij}^n, c_{ij}^n)\mathbf{v} + \left(\frac{\boldsymbol{D}}{s}\right)(\bar{s}_{ij}^n, c_{ij}^n)\nabla s\right)\Delta t/\phi,$$

where, as before, $\bar{\mathbf{x}}_{ij}^c$ is the origin point of the characteristics which reach $\mathbf{x}_{ij}^c$ at time t^{n+1}. Here the superscript 'c' is used to denote the characteristic curves associated with the polymer transport equation Eq. (16b). Thus we arrive at the following implicit-time finite difference formulation for Eq. (16b)

$$\phi \frac{c_{ij}^{n+1} - \bar{c}_{ij}^n}{\Delta t} + \frac{(g_1)_{ij}}{s_{ij}^n} c_{ij}^{n+1} = \frac{(g_2)_{ij}}{s_{ij}^n} \tag{21}$$

where $\bar{c}_{ij}^n = c(\bar{\mathbf{x}}_{ij}^c, t^n)$. Hence Eq. (20) and Eq. (21) form the finite difference approximation of the transport equations, Eq. (16a) and Eq. (16b) respectively.

The pseudocode (see Algorithm 1) for the method is given below.

Algorithm 1 Polymer flooding simulation

procedure

Set up Cartesian grid and FE Mesh and a permeability field

$i, j \leftarrow 1, \ldots, N;\ h \leftarrow \dfrac{1}{N}$ ▷ (*$N \times N$ is the grid size*)

$\Sigma \leftarrow$ *Initial interface* ▷ $\Sigma = \partial\Omega^+ \cup \partial\Omega^-$

$\mathbf{K}(\mathbf{x}) \leftarrow$ *choose type of heterogeneity*

Set model parameters

$\mu_o,\ \mu_w,\ s_{ro},\ s_{ra},\ \tilde{q} \leftarrow$ *values from Table 1*

Initialization

$s_0, c_0 \leftarrow \begin{cases} 1, 0 & x \in \Omega^+ \\ s_0, c_0 & x \in \Omega^- \end{cases}$

$t \leftarrow 0$

$\Delta t \leftarrow$ *value* ▷ Δt chosen for desired accuracy

Computation loop

while $(s(\mathbf{x}_{N,N}) \leq 1 - s_0)$ **do**

Compute $(\mu_a,\ \lambda_a,\ \lambda_o,\ \lambda,\ p_c)(s, c, \mathbf{v})$ using $(s^n, c^n, \mathbf{v}^{n-1})$

Solve the global pressure equation for p^n, v^n

Recompute $(s_{ra},\ s_{ro},\ \lambda_a,\ \lambda_o,\ \lambda)(s, c, \mathbf{v})$ using $(s^n, c^n, \mathbf{v}^n)$

Solve the transport equations for s^{n+1} and c^{n+1}

$t \leftarrow t + \Delta t$

close;

4 Convergence study and error analysis

For the convergence study, we choose the simple case of polymer flood in a one dimensional setting. The corresponding analysis for the full two dimensional surfactant polymer flood follows directly from this.

Let $s_i^n = s(x_i, t^n)$ be the grid values of the actual solution of the saturation equation, Eq. (16a) and let $w_i^n = w(x_i, t^n)$ be the grid values of the numerical solution of that equation where $x_i = ih$ and $t^n = n\Delta t$. Similarly let p_i^n, r_i^n be the grid values of the actual and numerical solution respectively of Eq. (12a); c_i^n, m_i^n be the grid values of the actual and numerical solution respectively of Eq. (16b) and v_i^n, z_i^n be the grid values of the actual and numerical solution respectively of the total velocity given by $\mathbf{v} = -\mathbf{K}\lambda\boldsymbol{\nabla}p$.
Let the errors in numerical approximation be given by the following:

$$\zeta_i^n = s_i^n - w_i^n, \quad \pi_i^n = p_i^n - r_i^n, \quad \theta_i^n = c_i^n - m_i^n.$$

We define the following discrete norms for any $u \in W^{l,p}(\Omega)$, $v \in l^2(\Omega)$ and $w \in l^\infty(\Omega)$ where $\Omega = [0, 1]^2$.

$$\|u\|_{l,p} = \left(\sum_{k=0}^{l}\left(\sum_i h\left|\frac{d^k u_i}{dx^k}\right|^p\right)\right)^{1/p}, \quad |u|_{l,p} = \left(\sum_i h\left|\frac{d^l u_i}{dx^l}\right|^p\right)^{1/p}$$

$$\|v\| = \left(\sum_i h|v_i|^2\right)^{1/2}$$

$$\|w\|_\infty = \max_i |w_i|$$

The reduced system of equations (see eqs. (16a) and (16b)) we consider in this analysis are

$$\phi\frac{\partial s}{\partial t}+b\frac{\partial s}{\partial x}+\frac{\partial}{\partial x}\left(D\frac{\partial s}{\partial x}\right)=F,\qquad s(x,0)=s_0(x);\quad x\in\Omega\setminus\partial\Omega \tag{22a}$$

$$\phi\frac{\partial c}{\partial t}+a\frac{\partial c}{\partial x}+Gc=H,\qquad c(x,0)=c_0(x);\quad x\in\Omega\setminus\partial\Omega \tag{22b}$$

where $\frac{\partial f}{\partial s}v=b(s,c)$, $(\frac{f}{s}v+\frac{D}{s}\frac{\partial s}{\partial x})=a(s,c)$. Also $F=g_1-\frac{\partial f}{\partial c}v\frac{\partial c}{\partial x}$, $G=g_1/s$ and $H=g_2/s$ are appropriate source terms. Then the characteristic finite difference approximation of Eq. (22a) and Eq. (22b) are given by,

$$\phi_i\frac{w_i^n-\bar{w}_i^{n-1}}{\Delta t}+\delta_x(\bar{D}\delta_x w^n)_i=F_i^n\qquad w_i^0=s_0(x_i), \tag{23}$$

$$\phi_i\frac{m_i^n-\bar{m}_i^{n-1}}{\Delta t}+G_i^n m_i^n=H_i^n\qquad m_i^0=c_0(x_i), \tag{24}$$

where $\bar{w}_i^{n-1}=w(\tilde{x}_i^s,t^{n-1})$, $\bar{m}_i^{n-1}=m(\tilde{x}_i^c,t^{n-1})$ and $\tilde{x}_i^s=x_i-b(w_i^{n-1},m_i^{n-1})\Delta t/\phi_i$, $\tilde{x}_i^c=x_i-a(w_i^n,m_i^{n-1})\Delta t/\phi_i$. From Eq. (22a) and Eq. (23) we have the following

$$\psi_s\frac{\partial s}{\partial\tau}+\frac{\partial}{\partial x}\left(D\frac{\partial s}{\partial x}\right)=F(s^n,c^n),\qquad s(x,0)=s_0(x); \tag{25a}$$

$$\phi_i\frac{w_i^n-\bar{w}_i^{n-1}}{\Delta t}+\delta_x(\bar{D}\delta_x w^n)_i=F(w_i^n,m_i^n)\qquad w_i^0=s_0(x_i). \tag{25b}$$

In the following analysis, M, M_k, C_k for $k\in\mathcal{Z}^+$ are generic constants independent of the time step and space discretizations Δt and h respectively. We will also assume the following bounds on the porosity, $\phi_*\le\phi(x)\le\phi^*$. For the rest of the analysis of the water saturation equation, we will be making a slight abuse of notation and writing $\tilde{x}_i^n$ and $\bar{x}_i^n$ to mean $\tilde{x}_i^{s,n}$ and $\bar{x}_i^{s,n}$ respectively. In the next two lemmas we compute the error in approximating the derivative in the characteristic direction and the second order derivative term using a finite difference discretization.

Lemma 4.1 *The error in approximating the derivative in the characteristic direction is given by*

$$\psi_{s,i}\left(\frac{\partial s}{\partial\tau}\right)_i^n-\phi_i\frac{s_i^n-\bar{s}_i^{n-1}}{\Delta t}=O\left(\left|\frac{\partial^2 s^*}{\partial\tau^2}\right|\Delta\tau\right).$$

where $\bar{s}_i^{n-1}=s(\bar{x}_i,t^{n-1})$ with $\bar{x}_i=x_i-b(s_i^n,c_i^n)\Delta t/\phi_i$.

Proof Let $p_1=(x,t^n)$ be a point on the grid and the characteristic that passes through this point intersects the previous time level at $p_2=(\bar{x},t^{n-1})$ where $\bar{x}=x-b(s,c)/\phi(x)\Delta t$ and let $\Delta\tau=\left[(x-\bar{x})^2+(t^n-t^{n-1})^2\right]^{1/2}$. Hence $\Delta\tau=\frac{\psi_s}{\phi}\Delta t$. Then using Taylor series expansion along the characteristic direction we write,

$$\begin{aligned}
&s(p_1-\Delta\tau)=s(p_1)-\Delta\tau\frac{\partial s}{\partial\tau}+\frac{\Delta\tau^2}{2}\frac{\partial^2 s}{\partial\tau^2}(p_1^*);\quad p_1^*\in(p_1,p_2)\\
&\Rightarrow\bar{s}^{n-1}=s^n-\Delta\tau\frac{\partial s^n}{\partial\tau}+\frac{\Delta\tau^2}{2}\frac{\partial^2 s}{\partial\tau^2}(p_1^*)\\
&\Rightarrow\Delta\tau\frac{\partial s^n}{\partial\tau}=s^n-\bar{s}^{n-1}+\frac{\Delta\tau^2}{2}\frac{\partial^2 s}{\partial\tau^2}(p_1^*)\\
&\Rightarrow\psi_s\frac{\partial s^n}{\partial\tau}-\phi\frac{s^n-\bar{s}^{n-1}}{\Delta t}=\frac{\phi}{\Delta t}\frac{\Delta\tau^2}{2}\frac{1}{2}\frac{\partial^2 s}{\partial\tau^2}(p_1^*)\quad\left(\because\frac{\psi_s}{\Delta\tau}=\frac{\phi}{\Delta t}\right)\\
&\qquad\qquad\qquad\qquad\qquad=\frac{\psi_s}{\Delta\tau}\frac{\Delta\tau^2}{2}\frac{\partial^2 s}{\partial\tau^2}(p_1^*)=\frac{\psi_s}{2}\Delta\tau\frac{\partial^2 s}{\partial\tau^2}(p_1^*)\\
&\therefore\quad\psi_{s,i}\left(\frac{\partial s}{\partial\tau}\right)_i^n-\phi_i\frac{s_i^n-\bar{s}_i^{n-1}}{\Delta t}=O\left(\left|\frac{\partial^2 s^*}{\partial\tau^2}\right|\Delta\tau\right).\quad\blacksquare
\end{aligned}$$

Using Lemma 4.1 in Eq. (25a) we estimate the error introduced by numerical discretization of the characteristic derivative as

$$\phi_i \frac{s_i^n - \bar{s}_i^{n-1}}{\Delta t} + \frac{\partial}{\partial x}\left(D\frac{\partial s^n}{\partial x}\right)_i = F(s_i^n, c_i^n) + O\left(\left|\frac{\partial^2 s^*}{\partial \tau^2}\right| \Delta\tau\right). \tag{26}$$

Now we turn our attention to the approximation error for the second order derivative term in the left hand side of Eq. (25a). By definition,

$$\begin{aligned}
\delta_x(\bar{D}\delta_x w^n)_i &= \frac{1}{h}\left(\bar{D}_{i+1/2}(\delta_x w^n)_{i+1/2} - \bar{D}_{i-1/2}(\delta_x w^n)_{i-1/2}\right) \\
&= \frac{1}{h^2}\left(\bar{D}_{i+1/2}(w_{i+1}^n - w_i^n) - \bar{D}_{i-1/2}(w_i^n - w_{i-1}^n)\right) \text{ where,} \\
\bar{D}_{i+1/2} &= \frac{1}{2}\left[D(x_i, \bar{w}_i^{n-1}) + D(x_{i+1}, \bar{w}_{i+1}^{n-1})\right] \\
\bar{D}_{i-1/2} &= \frac{1}{2}\left[D(x_i, \bar{w}_i^{n-1}) + D(x_{i-1}, \bar{w}_{i-1}^{n-1})\right]
\end{aligned}$$

The numerical approximation of the second order derivative in Eq. (22a) is given by

$$\begin{aligned}
\delta_x(D\delta_x s^n)_i &= \frac{1}{h^2}\left[D_{i+1/2}(s_{i+1}^n - s_i^n) - D_{i-1/2}(s_i^n - s_{i-1}^n)\right] \text{ where,} \\
D_{i+1/2} &= \frac{1}{2}\left[D(x_i, s_i^n) + D(x_{i+1}, s_{i+1}^n)\right] \\
D_{i-1/2} &= \frac{1}{2}\left[D(x_i, s_i^n) + D(x_{i-1}, s_{i-1}^n)\right]
\end{aligned}$$

Lemma 4.2 *The finite difference approximation error of the second derivative term is given by*

$$\frac{d}{dx}\left(D\frac{d}{dx}s^n\right)_i - \delta_x(D\delta_x s^n)_i = O(h\|s^n\|_{3,\infty}).$$

Proof From Taylor series expansion we know that

$$\begin{aligned}
\left(\frac{du}{dx}\right) - \frac{u(x+h/2) - u(x-h/2)}{h} &= O(h^2\|u\|_{3,\infty}) \\
\Rightarrow \left(\frac{du}{dx}\right)_i - \delta_x(u_i) &= O(h^2\|u\|_{3,\infty}) \\
\therefore \quad \frac{d}{dx}\left(D\frac{d}{dx}s^n\right)_i - \delta_x(D\delta_x s^n)_i &= O\left(h^2\left\|D\frac{d}{dx}s^n\right\|_{3,\infty}\right)
\end{aligned}$$

$$\Rightarrow \frac{d}{dx}\left(D\frac{d}{dx}s^n\right)_i - \frac{1}{h}\left(\left(D\frac{ds^n}{dx}\right)_{i+1/2} - \left(D\frac{ds^n}{dx}\right)_{i-1/2}\right) = O\left(h^2\left\|D\frac{d}{dx}s^n\right\|_{3,\infty}\right)$$

Since $(D\frac{ds^n}{dx})_{i+1/2} = D_{i+1/2}(\frac{ds^n}{dx})_{i+1/2} = D_{i+1/2}(\frac{s_{i+1}^n - s_i^n}{h}) + D_{i+1/2}O(h^2||s^n||_{3,\infty})$, we continue from above as

$$\begin{aligned}
&\frac{d}{dx}\left(D\frac{d}{dx}s^n\right)_i - \frac{1}{h}\left[D_{i+1/2}\frac{s_{i+1}^n - s_i^n}{h} + D_{i+1/2}O(h^2\|s^n\|_{3,\infty})\right] \\
&\quad + \frac{1}{h}\left[D_{i-1/2}\frac{s_i^n - s_{i-1}^n}{h} + D_{i-1/2}O(h^2\|s^n\|_{3,\infty})\right] = O\left(h^2\|D\|_{3,\infty}\left\|\frac{ds^n}{dx}\right\|_{3,\infty}\right)
\end{aligned}$$

Hence

$$\begin{aligned}
\frac{d}{dx}\left(D\frac{d}{dx}s^n\right)_i &- \frac{1}{h}\left[D_{i+1/2}\frac{s_{i+1}^n - s_i^n}{h} - D_{i-1/2}\frac{s_i^n - s_{i-1}^n}{h}\right] \\
&= D_{i+1/2}\, O(h\|s^n\|_{3,\infty}) - D_{i-1/2}\, O(h\|s^n\|_{3,\infty}) + O\left(h^2\|D\|_{3,\infty}\left\|\frac{ds^n}{dx}\right\|_{3,\infty}\right) \\
&= O(h\|s^n\|_{3,\infty}) + O(h^2\|s^n\|_{4,\infty}) = O(h\|s^n\|_{3,\infty}). \quad \blacksquare
\end{aligned}$$

Using the result of Lemma 4.2 we rewrite Eq. (26) as

$$\phi_i\frac{s_i^n - \bar{s}_i^{n-1}}{\Delta t} + \delta_x(D\delta_x s^n)_i = F(s_i^n, c_i^n) + O\left(\left|\frac{\partial^2 s^*}{\partial \tau^2}\right|\Delta\tau\right) + O(h\|s^n\|_{3,\infty}). \tag{27}$$

Subtracting Eq. (25b) from Eq. (27) we write,

$$\begin{aligned}
\phi_i\frac{s_i^n - \bar{s}_i^{n-1}}{\Delta t} - \phi_i\frac{w_i^n - \bar{w}_i^{n-1}}{\Delta t} &+ \delta_x(D\delta_x s^n)_i - \delta_x(\bar{D}\delta_x w^n)_i \\
&= F(s_i^n, c_i^n) - F(w_i^n, m_i^n) + O\left(\left|\frac{\partial^2 s^*}{\partial \tau^2}\right|\Delta\tau, h\|s^n\|_{3,\infty}\right)
\end{aligned}$$

Recall that we define the numerical error in saturation as $\zeta_i^n = s_i^n - w_i^n$. Using the definition of ζ_i^n and rearranging terms we rewrite the above as

$$\begin{aligned}
\phi_i\frac{\zeta_i^n - (\bar{s}_i^{n-1} - \bar{w}_i^{n-1})}{\Delta t} &+ \delta_x(\bar{D}\delta_x\zeta^n)_i = F(s_i^n, c_i^n) - F(w_i^n, m_i^n) \\
&+ O\left(\left|\frac{\partial^2 s^*}{\partial \tau^2}\right|\Delta\tau, h\|s^n\|_{3,\infty}\right) - \delta_x((D - \bar{D})\delta_x s^n)_i
\end{aligned} \tag{28}$$

We need to estimate the error terms ζ_i^n, θ_i^n and π_i^n which will also be useful for convergence analysis of the method.

We begin by considering the first term on the left hand side of Eq. (28). Let $\zeta^n = \mathcal{I}\zeta_i^n$ be the piecewise linear interpolant of ζ_i^n such that $\bar{\zeta}_i^{n-1} = \mathcal{I}\zeta^{n-1}(\tilde{x}_i) = \mathcal{I}s^{n-1}(\tilde{x}_i) - w^{n-1}(\tilde{x}_i) = \mathcal{I}s^{n-1}(\tilde{x}_i) - \bar{w}_i^{n-1}$. Then,

$$\begin{aligned}
\zeta_i^n - (\bar{s}_i^{n-1} - \bar{w}_i^{n-1}) &= (\zeta_i^n - \bar{\zeta}_i^{n-1}) + \mathcal{I}s^{n-1}(\tilde{x}_i) - \bar{w}_i^{n-1} - \bar{s}_i^{n-1} + \bar{w}_i^{n-1} \\
&= (\zeta_i^n - \bar{\zeta}_i^{n-1}) - \underbrace{(s^{n-1}(\bar{x}_i) - s^{n-1}(\tilde{x}_i))}_{\text{A}} - \underbrace{((1-\mathcal{I})s^{n-1}(\tilde{x}_i))}_{\text{B}}.
\end{aligned} \tag{29}$$

Below, we find estimates for the last two terms, A and B, of the right hand side of Eq. (29), followed by the estimate of the source term $(F(s_i^n, c_i^n) - F(w_i^n, m_i^n))$ on the right hand side of Eq. (28).

A. Estimate of the term A on the right hand side of Eq. (29): This is carried out in several steps below.

$$\begin{aligned}
& s^{n-1}(\bar{x}_1) - s^{n-1}(\tilde{x}_i) \\
& \le \hat{M}\|s^{n-1}\|_{1,\infty}\,|\bar{x}_i - \tilde{x}_i| \qquad (\hat{M} \text{ is a constant }) \\
& = \hat{M}\|s^{n-1}\|_{1,\infty}\left|\frac{\partial f}{\partial s}(w_i^{n-1}, m_i^{n-1})z_i^{n-1} - \frac{\partial f}{\partial s}(s_i^n, c_i^n)v_i^n\right|\frac{\Delta t}{\phi_i} \\
& \le \hat{M}\|s^{n-1}\|_{1,\infty}\left(\left|\frac{\partial f}{\partial s}(w_i^{n-1}, m_i^{n-1})\right|\underbrace{|z_i^{n-1} - v_i^n|}_{\text{A-1}}\right. \\
& \qquad \left. + |v_i^n|\underbrace{\left|\frac{\partial f}{\partial s}(w_i^{n-1}, m_i^{n-1}) - \frac{\partial f}{\partial s}(s_i^n, c_i^n)\right|}_{\text{A-2}}\right)\frac{\Delta t}{\phi_i}.
\end{aligned} \tag{30}$$

Next we estimate the terms A-1 and A-2 of the right hand side of (30).

A-1. Estimate of the term A-1 on the right hand side of Eq. (30):

We rewrite the term A-1 as

$$|z_i^{n-1} - v_i^n| \leq \underbrace{|z_i^{n-1} - v_i^{n-1}|}_{\text{A-1-I}} + \underbrace{|v_i^n - v_i^{n-1}|}_{\text{A-1-II}} \tag{31}$$

Recall that $z_i^n = -K\lambda(w_i^n, m_i^n)\frac{\partial r_i^n}{\partial x}$ and $v_i^n = -K\lambda(s_i^n, c_i^n)\frac{\partial p_i^n}{\partial x}$. Then the first term A-1-I on the right hand side of the above inequality (31) is written as

$$\begin{aligned}
|z_i^{n-1} - v_i^{n-1}| &= K\lambda(w_i^{n-1}, m_i^{n-1})\frac{\partial}{\partial x}(p_i^{n-1} - r_i^{n-1}) \\
&\quad + K\left(\lambda(s_i^{n-1}, c_i^{n-1}) - \lambda(w_i^{n-1}, m_i^{n-1})\right)\frac{\partial p_i^{n-1}}{\partial x} \\
&\leq \|K\|_\infty \|\lambda\|_\infty \left\|\frac{\partial}{\partial x}(\pi_i^{n-1})\right\|_\infty \\
&\quad + \|K\|_\infty \left|\lambda(s_i^{n-1}, c_i^{n-1}) - \lambda(w_i^{n-1}, m_i^{n-1})\right| \left\|\frac{\partial}{\partial x}(p_i^{n-1})\right\|_\infty .
\end{aligned} \tag{32}$$

The non-traditional discontinuous finite element method adopted here for solving the pressure equation gives us the following estimates [30],

$$\left\|\frac{\partial \pi^n}{\partial x}\right\|_\infty = O(h). \tag{33}$$

The numerical scheme will still converge if a different finite element formulation is used as long as it preserves or improves upon the above error estimate. Using Taylor series we write,

$$\begin{aligned}
|\lambda(s_i^{n-1}, c_i^{n-1}) - \lambda(w_i^{n-1}, m_i^{n-1})| &\leq |s_i^{n-1} - w_i^{n-1}| \left\|\frac{\partial \lambda}{\partial s}\right\|_\infty + |c_i^{n-1} - m_i^{n-1}| \left\|\frac{\partial \lambda}{\partial c}\right\|_\infty \\
&\leq \bar{M}(|\zeta_i^{n-1}| + |\theta_i^{n-1}|)
\end{aligned} \tag{34}$$

Using Eq. (33) and Eq. (34) in Eq. (32), we obtain following estimate for the first term A-1-I of the righthand side of (31).

$$|z_i^{n-1} - v_i^{n-1}| \leq M(h + |\zeta_i^{n-1}| + |\theta_i^{n-1}|) \tag{35}$$

To estimate the term A-1-II of the inequality (31) we observe

$$|v_i^n - v_i^{n-1}| \leq \Delta t \left\|\frac{\partial v}{\partial t}\right\|. \tag{36}$$

Using Eq. (35) and Eq. (36) in (31), we obtain the following estimate for A-1 (see Eq. (30)).

$$|z_i^{n-1} - v_i^n| \leq M(h + \Delta t + |\zeta_i^{n-1}| + |\theta_i^{n-1}|). \tag{37}$$

This concludes the estimate for the term A-1 in Eq. (30).

A-2. Estimate of the term A-2 on the right hand side of Eq. (30):

$$\begin{aligned}
&\left|\frac{\partial f}{\partial s}(w_i^{n-1}, m_i^{n-1}) - \frac{\partial f}{\partial s}(s_i^n, c_i^n)\right| \\
&\leq \left|(w_i^{n-1} - s_i^{n-1})\right| \left\|\frac{\partial^2 f}{\partial s^2}\right\|_\infty + \left|m_i^{n-1} - c_i^{n-1}\right| \left\|\frac{\partial^2 f}{\partial c\,\partial s}\right\|_\infty \\
&\qquad + \left|s_i^{n-1} - s_i^n\right| \left\|\frac{\partial^2 f}{\partial s^2}\right\|_\infty \left\|\frac{\partial s}{\partial t}\right\|_\infty + \left|c_i^{n-1} - c_i^n\right| \left\|\frac{\partial^2 f}{\partial c\,\partial s}\right\|_\infty \left\|\frac{\partial c}{\partial t}\right\|_\infty \\
&\leq M(|\zeta_i^{n-1}| + |\theta_i^{n-1}| + \Delta t)
\end{aligned} \tag{38}$$

Using the estimates for A-1 and A-2, as given by Eq. (37) and Eq. (38) respectively, in Eq. (30) we finally obtain the estimate for the term A of Eq. (29) as

$$|s^{n-1}(\bar{x}_i) - s^{n-1}(\tilde{x}_i)| \le M\Delta t(|\zeta_i^{n-1}| + |\theta_i^{n-1}| + h + \Delta t) \tag{39}$$

B. Estimate of the term B on the right hand side of Eq. (29):

Using the Peano kernel Theorem,[15] we obtain the following,

$$(1 - \mathcal{I})s^{n-1}(\tilde{x}_i) = O(h^2 \|s^{n-1}\|_{2,\infty}) \tag{40}$$

C. Estimate of the source term $(F(s_i^n, c_i^n) - F(w_i^n, m_i^n))$ in Eq. (28):

$$\begin{aligned} F(s_i^n, c_i^n) - F(w_i^n, m_i^n) &\le |s_i^n - w_i^n| \left\| \frac{\partial F}{\partial s} \right\|_\infty + |c_i^n - m_i^n| \left\| \frac{\partial F}{\partial c} \right\|_\infty \\ &\le M(|\zeta_i^n| + |\theta_i^n|) \end{aligned} \tag{41}$$

Using the estimates (39) and (40) in (29) first and then using the resulting (29) and (41) in (28), we obtain

$$\begin{aligned} \underbrace{\phi_i \frac{\zeta_i^n - \bar{\zeta}_i^{n-1}}{\Delta t}}_{\text{D-1}} + \underbrace{\delta_x(D\delta_x\zeta^n)_i}_{\text{D-2}} &\le M\left(h + \Delta t + h^2/\Delta t + |\zeta_i^{n-1}| + |\theta_i^{n-1}| + |\zeta_i^n| + |\theta_i^n|\right) \\ &+ \underbrace{\epsilon_i^n}_{\text{D-3}} - \underbrace{\delta_x[(D - \bar{D})\delta_x s^n]_i}_{\text{D-4}} \end{aligned} \tag{42}$$

where $\epsilon_i^n = O(\|\frac{\partial^2 s}{\partial \tau^2}\|_\infty \Delta\tau, \|s^n\|_{3,\infty} h)$. Below, we test Eq. (42) against ζ_i^n and obtain the estimates for the inner products involving the terms D-1, D-2, D-3 and D-4.

D-1. Estimate of the term D-1: The inner product is rewritten as

$$\langle \phi_i \frac{\zeta_i^n - \bar{\zeta}_i^{n-1}}{\Delta t}, \zeta_i^n \rangle = \underbrace{\langle \phi_i \frac{\zeta_i^n - \zeta_i^{n-1}}{\Delta t}, \zeta_i^n \rangle}_{\text{D-1-1}} - \langle \phi_i \frac{\bar{\zeta}_i^{n-1} - \zeta_i^{n-1}}{\Delta t}, \zeta_i^n \rangle$$

Using the inequality $|a - b||a| \ge \dfrac{|a|^2 - |b|^2}{2}$ we estimate the term D-1-1 as

$$\langle \phi_i \frac{\zeta_i^n - \zeta_i^{n-1}}{\Delta t}, \zeta_i^n \rangle \ge \frac{M}{\Delta t}(\|\zeta^n\|^2 - \|\zeta^{n-1}\|^2)$$

D-2. Estimate of the term D-2 in Eq. (42): Testing the term D-2 against ζ_i^n and using summation by parts we write

$$\langle \delta_x(D\delta_x\zeta^n)_i, \zeta_i^n \rangle = -\langle (D\delta_x\zeta^n)_i, (\delta_x\zeta^n)_i \rangle$$

and similarly for D-4 we have

$$\langle \delta_x((d - \bar{D})\delta_x s^n)_i, \zeta_i^n \rangle = -\langle ((D - \bar{D})\delta_x s^n)_i, (\delta_x\zeta^n)_i \rangle.$$

D-3. Estimate of the term D-3 in Eq. (42): Finally testing the term D-3 against ζ_i^n we get

$$\langle \epsilon_i^n, \zeta_i^n \rangle \le M(h + \Delta t) \sum_i h|\zeta_i^n| \le M(h^2 + \Delta t^2 + \|\zeta^n\|^2)$$

Substituting the estimates for the term D-1-1 and the inner products involving the terms D-2, D-3 and D-4 in Eq. (42) we rewrite it as,

$$\frac{M}{\Delta t}(\|\zeta^n\|^2 - \|\zeta^{n-1}\|^2) - \underbrace{\langle (D\delta_x\zeta^n)_i, (\delta_x\zeta^n)_i\rangle}_{\text{E-1}} \le \hat{M}\Big(\|\zeta^n\|^2 + \underbrace{\langle\theta_i^n, \zeta_i^n\rangle}_{\text{E-2}} + h^2 + \Delta t^2$$
$$+ \|\zeta^{n-1}\|^2 + \|\theta^{n-1}\|^2\Big) + \underbrace{\langle((D-\bar{D})\delta_x s^n)_i, (\delta_x\zeta^n)_i\rangle}_{\text{E-3}} + \underbrace{\langle\phi_i \frac{\bar{\zeta}_i^{n-1} - \zeta_i^{n-1}}{\Delta t}, \zeta_i^n\rangle}_{\text{E4}} \tag{43}$$

We now estimate the remaining inner product terms in Eq. (43).

$$\begin{aligned}
&\textbf{E-1}: \quad -\langle (D\delta_x\zeta^n)_i, (\delta_x\zeta^n)_i\rangle \ge -D^*|\zeta^n|_{1,2}^2,\\
&\textbf{E-2}: \quad \langle\theta_i^n, \zeta_i^n\rangle \le M(\|\theta^n\|^2 + \|\zeta^n\|^2) \text{ (using Cauchy-Schwarz) },\\
&\textbf{E-3}: \quad \langle((D-\bar{D})\delta_x s^n)_i, (\delta_x\zeta^n)_i\rangle = \sum_i h|(D-\bar{D})\delta_x s^n|_i |\delta_x\zeta^n|_i\\
&\qquad\qquad \le \left\|\frac{\partial s_i^n}{\partial x}\right\|_\infty \sum_i h\big|D(s_i^n, c_i^n) - D(w_i^{n-1}, m_i^{n-1})\big|\left|\frac{\partial\zeta_i^n}{\partial x}\right|.
\end{aligned}$$

Using Taylor series we write

$$\begin{aligned}
\big|D(s_i^n, c_i^n) - D(w_i^{n-1}, m_i^{n-1})\big| &\le |s_i^n - w_i^{n-1}|\left\|\frac{\partial D}{\partial s}\right\|_\infty + |c_i^n - m_i^{n-1}|\left\|\frac{\partial D}{\partial c}\right\|_\infty\\
&\le M(|\zeta_i^{n-1}| + |\theta_i^{n-1}| + \Delta t),
\end{aligned}$$

where we use the estimate

$$|s_i^n - w_i^{n-1}| \le |s_i^n - s_i^{n-1}| + |s_i^{n-1} - w_i^{n-1}| \le M(|\zeta_i^{n-1}| + \Delta t)$$

and similarly $|c_i^n - m_i^{n-1}| \le M(|\theta_i^{n-1}| + \Delta t)$. Hence we have an estimate for E-3 as,

$$\begin{aligned}
&\langle((D-\bar{D})\delta_x s^n)_i, (\delta_x\zeta^n)_i\rangle \le M_1\|s^n\|_{1,\infty}\sum_i h|\zeta_i^{n-1}|\left|\frac{\partial\zeta_i^n}{\partial x}\right|\\
&\qquad + M_2\|s^n\|_{1,\infty}\sum_i h|\theta_i^{n-1}|\left|\frac{\partial\zeta_i^n}{\partial x}\right| + (M_1+M_2)\|s^n\|_{1,\infty}\sum_i h\Delta t\left|\frac{\partial\zeta_i^n}{\partial x}\right|\\
&\le M(\|\zeta^{n-1}\|^2 + \|\theta^{n-1}\|^2 + |\zeta^n|_{1,2}^2 + \Delta t^2).
\end{aligned}$$

E-4. Estimate of the term E-4 in Eq. (43): Using the fundamental theorem of calculus,

$$\bar{\zeta}_i^{n-1} - \zeta_i^{n-1} = \int_{x_i}^{\tilde{x_i}} \frac{\partial\zeta^{n-1}}{\partial x}\frac{\tilde{x}_i - x_i}{|\tilde{x}_i - x_i|}\,d\sigma$$

$$\text{Hence} \quad |\bar{\zeta}_i^{n-1} - \zeta_i^{n-1}| \le \int_{x_i}^{\tilde{x_i}}\left|\frac{\partial\zeta^{n-1}}{\partial x}\right|d\sigma \le \left(\int_{x_i}^{\tilde{x_i}} d\sigma\right)^{1/2}\left(\int_{x_i}^{\tilde{x_i}}\left|\frac{\partial\zeta^{n-1}}{\partial x}\right|d\sigma\right)^{1/2}.$$

Therefore,

$$\begin{aligned}
\langle\phi_i\frac{\bar{\zeta}_i^{n-1} - \zeta_i^{n-1}}{\Delta t}, \zeta_i^n\rangle &\le \frac{\phi^*}{\Delta t}\left(\sum_i h|\zeta_i^n|^2\right)^{1/2}\left(\sum_i h|\bar{\zeta}_i^{n-1} - \zeta_i^{n-1}|^2\right)^{1/2}\\
&\le M|\zeta^{n-1}|_{1,2}|\zeta^n|_\infty\\
&\le M|\zeta^{n-1}|_{1,2}|\zeta^n|_{1,2}(\log 1/h)^{1/2} \quad \text{[Using a result from [32]]}\\
&\le M(\log 1/h)^{1/2}\left(|\zeta^{n-1}|_{1,2}^2 + |\zeta^n|_{1,2}^2\right).
\end{aligned}$$

Above we have used that $\|z^{n-1}\|_\infty$ is bounded which has been proved below after Eq. (54). Using all of the above estimates for E-1, E-2, E-3, E-4 in Eq. (43) we get,

$$\begin{aligned}(M-\epsilon)(\|\zeta^n\|^2 - \|\zeta^{n-1}\|^2) + \epsilon(\|\theta^n\|^2 - \|\theta^{n-1}\|^2) - D^*\Delta t|\zeta^n|_{1,2}^2 \\ \leq \epsilon(h^2+\Delta t^2) + \epsilon(1+(\log 1/h)^{1/2})\left(|\zeta^{n-1}|_{1,2}^2 + |\zeta^n|_{1,2}^2\right),\end{aligned}$$

where $\epsilon = M\Delta t$ is a very small positive number. Summing over $1 \leq n \leq L$ we get,

$$\begin{aligned}&(M-\epsilon)(\|\zeta^L\|^2 - \|\zeta^0\|^2) + \epsilon(\|\theta^0\|^2 - \|\theta^L\|^2) - D^*\Delta t\sum_{n=1}^{L}|\zeta^n|_{1,2}^2 \\ &\leq L\epsilon(h^2+\Delta t^2) + \epsilon\left(1+(\log 1/h)^{1/2}\right)\left(|\zeta^0|_{1,2}^2 + |\zeta^L|_{1,2}^2\right) \\ &\qquad + 2\epsilon\left(1+(\log 1/h)^{1/2}\right)\sum_{n=1}^{L-1}|\zeta^n|_{1,2}^2.\end{aligned}$$

Noting that $\zeta_i^0 = 0$ and $\theta_i^0 = 0$ we rewrite this as

$$(M-\epsilon)\|\zeta^L\|^2 - \epsilon\|\theta^L\|^2 - (D^*\Delta t + \rho_1)\sum_{n=1}^{L}|\zeta^n|_{1,2}^2 \leq \rho_2|\zeta^0|_{1,2}^2 + \bar{\epsilon}(h^2+\Delta t^2) \tag{44}$$

where $\bar{\epsilon} = L\epsilon$, $\rho_1 = \epsilon(1+(\log 1/h)^{1/2}) \to 0$ as $(h,\Delta t) \to 0$ and so does ρ_2. This concludes the analysis of the water transport equation (Eq. (22a)).

Next we consider the polymer transport equation (Eq. (22b)). Replacing the advective terms with a derivative along the characteristic direction, Eq. (22b) becomes

$$\psi_c\frac{\partial c}{\partial \tau} + Gc = H, \tag{45}$$

whose finite difference approximation is given by

$$\phi_i\frac{m_i^n - \bar{m}_i^{n-1}}{\Delta t} + G_i^n m_i^n = H_i^n. \tag{46}$$

Recall that $\theta_i^n = c_i^n - m_i^n$. Using an analogue of Lemma 4.1 for the characteristic derivative of the polymer transport equation in Eq. (45) and subtracting Eq. (46) from the result we get,

$$\begin{aligned}\phi_i\frac{\theta_i^n - (\bar{c}_i^{n-1} - \bar{m}_i^{n-1})}{\Delta t} + G_i^n\theta_i^n &= H(s_i^n) - H(w_i^n) + O\left(\left\|\frac{\partial^2 c}{\partial\tau^2}\right\|_\infty \Delta\tau\right) \\ &\leq |H(s_i^n) - H(w_i^n)| + M\Delta t\end{aligned} \tag{47}$$

As before the source terms are estimated as

$$|H(s_i^n) - H(w_i^n)| \leq |s_i^n - w_i^n|\left\|\frac{\partial H}{\partial s}\right\|_\infty \leq M|\zeta_i^n| \tag{48}$$

In the following, we will again slightly abuse notation and suppress the superscript "c" from $\tilde{x}_i^{c,n}$ and $\bar{x}_i^{c,n}$ to denote the points on the characteristic curves of the polymer equation. Continuing with the analysis, we rewrite the numerator of the first term of Eq. (47) on the left side as

$$\theta_i^n - (\bar{c}_i^{n-1} - \bar{m}_i^{n-1}) = (\theta_i^n - \bar{\theta}_i^{n-1}) - \underbrace{(c^{n-1}(\bar{x}_i) - c^{n-1}(\tilde{x}_i))}_{\text{F}} - \underbrace{(1-\mathcal{I})c^{n-1}(\tilde{x}_i)}_{\text{G}} \tag{49}$$

The term G is estimated by the Peano kernel theorem, as was done in Eq. (40).

F. Estimate of the term F: This estimate is carried out in a series of steps,

$$
\begin{aligned}
|c^{n-1}(\bar{x_i}) - c^{n-1}(\tilde{x_i})| &\le \|c^{n-1}\|_{1,\infty}|\tilde{x_i} - \bar{x_i}| \\
&\le M\frac{\Delta t}{\phi_*}\underbrace{\left|\frac{f}{s}(w_i^n, m_i^{n-1})z_i^{n-1} - \frac{f}{s}(s_i^n, c_i^n)v_i^n\right|}_{\text{F-1}} \\
&\qquad + M\frac{\Delta t}{\phi_*}\underbrace{\left|\frac{D}{s}(\bar{w}_i^n, m_i^{n-1})\frac{\partial w_i^n}{\partial x} - \frac{D}{s}(s_i^n, c_i^n)\frac{\partial s_i^n}{\partial x}\right|}_{\text{F-2}}
\end{aligned}
\tag{50}
$$

F-1. Estimate of the term F-1:

$$
\begin{aligned}
\left|\frac{f}{s}(w_i^n, m_i^{n-1})z_i^{n-1} - \frac{f}{s}(s_i^n, c_i^n)v_i^n\right| &\le \left|\frac{f}{s}(w_i^n, m_i^{n-1})\right|\underbrace{|z_i^{n-1} - v_i^n|}_{\text{F-1-1}} \\
&\qquad + \underbrace{\left|\frac{f}{s}(w_i^n, m_i^{n-1}) - \frac{f}{s}(s_i^n, c_i^n)\right|}_{\text{F-1-2}}|v_i^n|
\end{aligned}
\tag{51}
$$

Out of the two pieces F-1-1 and F-1-2 required to obtain an estimate of F-1, we have already estimated the term F-1-1 in Eq. (37) which we recall here: $\left|z_i^{n-1} - v_i^n\right| \le M(h + \Delta t + |\zeta_i^{n-1}| + |\theta_i^{n-1}|)$.

F-1-2. Estimate of the term F-1-2 in Eq. (51):

$$
\begin{aligned}
&\left|\frac{f}{s}(w_i^n, m_i^{n-1}) - \frac{f}{s}(s_i^n, c_i^n)\right| \\
&\qquad \le |\theta_i^{n-1}|\left\|\frac{\partial}{\partial c}\left(\frac{f}{s}\right)\right\|_\infty + |\zeta_i^n|\left\|\frac{\partial}{\partial s}\left(\frac{f}{s}\right)\right\|_\infty + \Delta t\left\|\frac{\partial c_i^n}{\partial t}\right\|_\infty\left\|\frac{\partial}{\partial c}\left(\frac{f}{s}\right)\right\|_\infty \\
&\qquad \le M(|\theta_i^{n-1}| + |\zeta_i^n| + \Delta t)
\end{aligned}
$$

Using these estimates of the terms F-1-1 and F-1-2 in the estimate of F-1, we obtain

$$
\left|\frac{f}{s}(w_i^n, m_i^{n-1})z_i^{n-1} - \frac{f}{s}(s_i^n, c_i^n)v_i^n\right| \le M(h + \Delta t + |\zeta_i^n| + |\zeta_i^{n-1}| + |\theta_i^{n-1}|)
\tag{52}
$$

F-2. Estimate of the term F-2 of Eq. (50):

$$
\begin{aligned}
&\left|\frac{D}{s}(\bar{w}_i^n, m_i^{n-1})\frac{\partial w_i^n}{\partial x} - \frac{D}{s}(s_i^n, c_i^n)\frac{\partial s_i^n}{\partial x}\right| \\
&\qquad \le \left(\underbrace{|\bar{w}_i^n - s_i^n|}_{\text{F-2-1}}\left\|\frac{\partial}{\partial s}\left(\frac{D}{s}\right)\right\|_\infty + |m_i^{n-1} - c_i^n|\left\|\frac{\partial}{\partial c}\left(\frac{D}{s}\right)\right\|_\infty\right)\left|\frac{\partial s_i^n}{\partial x}\right| \\
&\qquad\qquad + \left\|\frac{D}{s}(\bar{w}_i^n, m_i^{n-1})\right\|_\infty\left|\frac{\partial \zeta_i^n}{\partial x}\right|
\end{aligned}
\tag{53}
$$

F-2-1. Estimate of the term F-2-1:

$$
\bar{w}_i^n - s_i^n = \mathcal{I}s^n(\tilde{x}_i) - s^n(x_i) - \bar{\zeta}_i^n = (\tilde{x}_i - x_i)\frac{\partial s^{n*}}{\partial x} - (\mathcal{I} - 1)s^n(\tilde{x}_i) - \bar{\zeta}_i^n
$$

Therefore

$$
\begin{aligned}
|\bar{w}_i^n - s_i^n| &\leq |\tilde{x}_i - x_i| \, \|s^n\|_{1,\infty} + Ch^2 + |\bar{\zeta}_i^n| \quad \text{(Using Peano-Kernel theorem)} \\
&\leq M\Delta t \left\{ \left\| \frac{f}{s} \right\|_\infty \|z^{n-1}\|_\infty + \left\| \frac{D}{s} \right\|_\infty \left(\left| \frac{\partial s_i^n}{\partial x} \right|_\infty + \left| \frac{\partial \zeta_i^n}{\partial x} \right| \right) \right\} + Ch^2 + |\bar{\zeta}_i^n| \\
&\leq M\Delta t \left\{ h + C + \left| \frac{\partial \zeta_i^n}{\partial x} \right| \right\} + Mh^2 + |\bar{\zeta}_i^n| \qquad (54)
\end{aligned}
$$

The last step of the above estimate in Eq. (54) requires a bound on $\|z^{n-1}\|_\infty$, which was also used while estimating the term E-4. Before moving further we prove this statement. Note that, even though we prove the result for $\|z^n\|_\infty$, it will be true for any other time, t^n with $n \in (0, T)$.

$$
\begin{aligned}
z_i^n = -K\lambda(w_i^n, m_i^n) \frac{\partial r_i^n}{\partial x} &= K\lambda(w_i^n, m_i^n) \left[\frac{\partial \pi_i^n}{\partial x} - \frac{\partial p_i^n}{\partial x} \right] \\
\|z^n\|_\infty \leq \|K\|_\infty \|\lambda\|_\infty \left(1 + \left\| \frac{\partial \pi_i^n}{\partial x} \right\|_\infty \right) &\leq M(1 + \beta h); \quad (\beta \text{ is a constant})
\end{aligned}
$$

Using the estimate for F-2-1 given in Eq. (54) in Eq. (53), we obtain

$$
\begin{aligned}
\left| \frac{D}{s}(\bar{w}_i^n, m_i^{n-1}) \frac{\partial w_i^n}{\partial x} - \frac{D}{s}(s_i^n, c_i^n) \frac{\partial s_i^n}{\partial x} \right| &\leq M \left(|\bar{w}_i^n - s_i^n| + |\theta_i^{n-1}| + \Delta t + \left| \frac{\partial \zeta_i^n}{\partial x} \right| \right) \\
&\leq M \left(\Delta t \left(h + C + \left| \frac{\partial \zeta_i^n}{\partial x} \right| \right) + h^2 + C|\bar{\zeta}_i^n| + |\theta_i^{n-1}| + \Delta t + \left| \frac{\partial \zeta_i^n}{\partial x} \right| \right) \\
&\leq M \left(h^2 + \Delta t + |\bar{\zeta}_i^n| + |\theta_i^{n-1}| + (1 + \Delta t) \left| \frac{\partial \zeta_i^n}{\partial x} \right| \right) \qquad (55)
\end{aligned}
$$

Using Eq. (52) and Eq. (55) in Eq. (50) we obtain the following estimate for the term B in Eq. (49).

$$
\begin{aligned}
|c^{n-1}(\bar{x}_i) - c^{n-1}(\tilde{x}_i)| &\leq M\Delta t \left(h + \Delta t + |\zeta_i^n| + |\zeta_i^{n-1}| + |\theta_i^{n-1}| \right) \\
&\quad + M\Delta t \left(h^2 + \Delta t + |\theta_i^{n-1}| + |\bar{\zeta}_i^n| + (1 + \Delta t) \left| \frac{\partial \zeta_i^n}{\partial x} \right| \right) \\
&\leq M\Delta t \left(h + \Delta t + |\zeta_i^n| + |\zeta_i^{n-1}| + |\theta_i^{n-1}| + |\bar{\zeta}_i^n| + (1 + \Delta t) \left| \frac{\partial \zeta_i^n}{\partial x} \right| \right) \qquad (56)
\end{aligned}
$$

Using Eq. (48) and Eq. (56), we rewrite Eq. (47) in terms of the error θ_i^n as

$$
\begin{aligned}
&\phi_* \frac{\theta_i^n - \bar{\theta}_i^{n-1}}{\Delta t} + \hat{M}\theta_i^n \\
&\qquad \leq M\Delta t \left(h + h^2 + \Delta t + |\zeta_i^n| + |\zeta_i^{n-1}| + |\theta_i^{n-1}| + |\bar{\zeta}_i^n| + (1 + \Delta t) \left| \frac{\partial \zeta_i^n}{\partial x} \right| \right)
\end{aligned}
$$

As shown before, in order to find estimates of the error norms we test the above equation against θ_i^n and after some simplification we get,

$$
\begin{aligned}
M(\|\theta^n\|^2 - \|\theta^{n-1}\|^2) &\leq \bar{M}\Delta t \left[|\theta^{n-1}|_{1,2}^2 + |\theta^n|_{1,2}^2 \right] (\log 1/h)^{1/2} \left(M_1 + \left\| \frac{\partial \zeta^n}{\partial x} \right\|_\infty \right) \\
&\quad + \tilde{M}\Delta t^2 \left(1 + h^2 + \Delta t^2 + \|\theta^n\|^2 + \|\zeta^n\|^2 + \|\theta^{n-1}\|^2 + \|\theta^{n-1}\|^2 + \|\bar{\zeta}^n\|^2 \right) \\
&\quad + \tilde{M}\Delta t^2 (1 + \Delta t) \left(\|\theta^n\|^2 + \left\| \frac{\partial \theta^n}{\partial x} \right\|^2 \right)
\end{aligned}
$$

Summing the above equation over $1 \leq n \leq L$ and using $\theta_i^0 = 0$ we get,

$$
\begin{aligned}
(M-\epsilon)\|\theta^L\|^2 \leq \rho_3 \left(\sum_{n=0}^{L} |\theta^n|_{1,2}^2\right) + \rho_3 (\log 1/h)^{1/2} \max_{1 \leq n \leq L} \|\zeta^n\|_\infty \left(\sum_{n=0}^{L} |\theta^n|_{1,2}^2\right) \\
+\epsilon(1+h^2+\Delta t^2) + \epsilon \left(\sum_{n=1}^{L} (\|\zeta^n\|^2 + \|\bar{\zeta}^n\|^2 + |\zeta^n|_{1,2}^2)\right),
\end{aligned} \tag{57}
$$

where $\rho_3 = M\Delta t(\log 1/h)^{1/2}$. Hence $\rho_3 \to 0$ and $\rho_3(\log 1/h)^{1/2} \to 0$ as $(h, \Delta t) \to 0$. Combining Eq. (44) and Eq. (57) we get the following convergence result.

Theorem 4.3 *Let the exact solutions of Eq.* (22a) *and Eq.* (22b) *have sufficient regularity. The difference scheme given by Eq.* (24) *and Eq.* (25b) *converges to the actual solution if* $\Delta t = O(h)$.

5 Numerical results

In this section we present numerical results to illustrate the efficiency and accuracy of this new hybrid method in solving the system of equations eqs. (7a)–(7c), subject to realistic initial and boundary data. In section 5.1 the input data given in table 1 is used for a quarter-five spot polymer flood. The numerical errors are measured in the discrete norms:

$$
e_{s,max} = \max_{ij} |s(\mathbf{x}_{ij}) - w_{ij}| \approx \|s - w\|_{L^\infty}, \tag{58a}
$$

$$
e_{s,2} = \sqrt{\sum_{ij} |s(\mathbf{x}_{ij}) - w_{ij}|^2 \Delta x \Delta y} \approx \|s - w\|_{L^2}. \tag{58b}
$$

Here, w_{ij} is the numerical solution w evaluated at the grid point $(x_i, y_j) = \mathbf{x}_{ij}$ whereas $s(\mathbf{x}_{ij})$ is the finest grid numerical solution in section 5.1. The errors for the pressure and the velocity are computed in a similar fashion. The order of accuracy is computed using the formula $\log_2(e_\alpha(h)/e_\alpha(h/2))$ $(\alpha = 2, \infty)$.

5.1 Two-dimensional polymer flood problem

In this section, we simulate polymer flooding until breakthrough occurs, on a quarter five-spot homogeneous reservoir over the spatial domain, $\Omega = [0,1]^2$ with absolute permeability, $\mathbf{K} = 1$ and input parameters listed in Table 1. We compute the L^∞ and L^2 error norms for the numerical solution of saturation, pressure and

Table 1: Simulation input data

Model parameter	Symbol	Value
Spatial grid size	$h \times k$	variable
Porosity	ϕ	1
Initial resident water saturation	$s_0^{\sigma 0}$	0.21
Oil viscosity	μ_o	12.6
Pure water viscosity	μ_w	1.26
Residual aqueous phase saturation	s_{ra}	0.1
Residual oleic phase saturation	s_{ro}	0.3
Parameters of capillary pressure relation [eq. (11c)]	α_0, m	0.125, 2/3
Concentration of polymer in injected fluid	c_0	0.1
Injection rate	$\tilde{q}$	200
Time step size	Δt	1/50

velocity for a sequence of uniformly refined meshes using eq. (58), but with $s(\mathbf{x}_{ij})$ representing the solution on the finest grid size, $h = 1/128$. A similar procedure is applied to estimate the error norms and the order of accuracy for pressure and velocity. The numerical errors and the order of accuracy are presented in Table 2. This strongly validates the accuracy and the efficiency of the method. In Table 3 we present the numerical errors and convergence rates with respect to time step size refinement for the quarter five-spot flooding problem. We observe the following approximate order of accuracy in space:

$$\|p - r\|_{L^2} = O(h^2) \quad \& \quad \|\mathbf{v} - \boldsymbol{z}\|_{L^2} = O(h^2)$$

Table 2 shows that for a given fixed time-step, the errors decrease with refinement of the spatial mesh. However, for larger time steps (larger than 0.05) we find (data not shown here) that the time discretization error dominates the spatial discretization errors. This leads to an increase in the L^2 and L^∞ error norms and a reduction in the order of accuracy. The order of accuracy in the L^∞ norm of the error in saturation, as presented in the upper part of the last column of Table 2 can also be seen to reduce significantly with reduction in spatial grid size. This is the because the numerical solution attains a high accuracy, to the order of 10^{-5}, even at the largest spatial grid size used ($h = 1/8$). The error between the actual solution and the numerical solution does not improve much further and causes the loss in the order of accuracy.

The non-symmetric algebraic systems obtained by assembling the stiffness matrix of the finite element weak formulation, given by eq. (15), and the symmetric but sparse algebraic systems obtained by discretizing the transport equations, given by eqs. (20) and (21), are solved by a BICGstab iterative method with tolerance values in the range $10^{-6} - 10^{-9}$ and without any preconditioners. Apart from achieving high accuracy, there is one more important significance of choosing such ultra-low values of tolerance, specifically for solving the transport equations. It has been observed that the BICGstab solver converges to a solution with a relative residual of about 10^{-6} within the first two iterations for even moderately fine spatial resolution of $h = 1/32$. Hence, it becomes necessary to choose much lower levels of tolerance, in order to check the convergence rates with respect to spatial discretization for the water saturation. However, it is worth pointing out that there is a delicate balance involved in such a choice. If the tolerance is reduced even further from 10^{-9}, then the BICGstab iteration process may stagnate and fail to achieve desired relative residuals.

Table 3 shows the numerical errors and the order of accuracy for the saturation equation with respect to time for three choices of fixed spatial grid sizes, namely $h = 1/16, 1/32$ and $1/64$. The errors are computed at the final time $T = 1$. The results confirm that at least a first-order convergence rate in time can be obtained using this method. This compares favorably with results by others (see [33]) on similar types of problems. Additionally, we expect that with higher order time-stepping methods, the method will be able to preserve the accuracy and the expected second or third order convergence rates. It is also important to note that with a fixed time step, the accuracy of the method increases with decreasing spatial grid size which can also serve as a quick validation of the results presented in Table 2.

In Figure 2 snapshots of the water saturation profile are given at the same time level $t = 0.5$ for four different spatial grid resolutions. One can observe the increase in the quality and sharpness of the saturation profiles with grid refinement while preserving the accuracy of the solution. This provides a qualitative numerical validation that the method converges to the correct solution with grid refinement.

6 Conclusions

This paper analyzes a hybrid numerical method for solving a multicomponent, immiscible displacement problem in porous media with two incompressible fluid phases. Polymer flooding is considered to be the model problem in this study. The mathematical model for polymer flooding uses a global pressure (proposed in [1]), the wetting phase saturation and the component concentration as the primary variables. The numerical method is based on an extended finite element method for the discontinuous coefficient elliptic pressure equation and a modified method of characteristics in combination with a time implicit finite difference method for the transport equations. The convergence behavior of the numerical method is studied in detail. Numerical experiments are performed to simulate polymer flooding in a quarter five-spot geometry. The L^2

Table 2: Error and order for saturation, pressure and velocity at water breakthrough of a quarter five-spot polymer flooding simulation

	h	$\|s-w\|_{L^2}$	Order	$\|s-w\|_{L^\infty}$	Order
Saturation	1/8	4.39e−3	–	3.64e−2	–
	1/16	1.85e−3	1.247	1.76e−2	1.048
	1/32	7.84e−4	1.239	1.08e−2	0.704
	1/64	3.22e−4	1.284	6.86e−3	0.656
	h	$\|p-r\|_{L^2}$	Order	$\|p-r\|_{L^\infty}$	Order
Pressure	1/8	4.12e−3	–	1.61e−3	–
	1/16	9.30e−4	2.147	4.75e−4	1.761
	1/32	2.10e−4	2.147	1.35e−4	1.815
	1/64	3.85e−5	2.448	3.10e−5	2.123
	h	$\|\mathbf{v}-\mathbf{r}\|_{L^2}$	Order	$\|\mathbf{v}-\mathbf{r}\|_{L^\infty}$	Order
Velocity	1/8	1.18e−3	–	6.941e−3	–
	1/16	2.94e−4	2.005	2.98e−3	1.220
	1/32	7.46e−5	1.979	1.39e−3	1.110
	1/64	1.96e−5	1.928	6.89e−4	1.002

Table 3: Error and rates for saturation with time step refinement at water breakthrough of a quarter five-spot polymer flooding simulation.

Δt	$h=1/16$		$h=1/32$		$h=1/64$	
	$\|s-w\|_{L^2}$	Rate	$\|s-w\|_{L^2}$	Rate	$\|s-w\|_{L^2}$	Rate
1/20	9.34e−3	–	8.93e−3	–	6.50e−3	–
1/40	4.36e−3	1.100	4.69e−3	0.923	3.48e−3	0.901
1/80	2.27e−3	0.941	2.51e−3	0.899	1.94e−3	0.846
1/160	1.25e−3	0.867	1.48e−3	0.762	1.17e−3	0.722

and L^∞ error norms are computed to demonstrate the numerical convergence and the order of accuracy of the method.

Acknowledgements

Numerical simulations were performed using high performance research computing resources provided by Texas A&M University (`http://hprc.tamu.edu`). The research reported in this paper was supported in part by the U.S. National Science Foundation grant DMS-1522782 and in part by the NPRP grant 08-777-1-141 through Qatar National Research Fund.

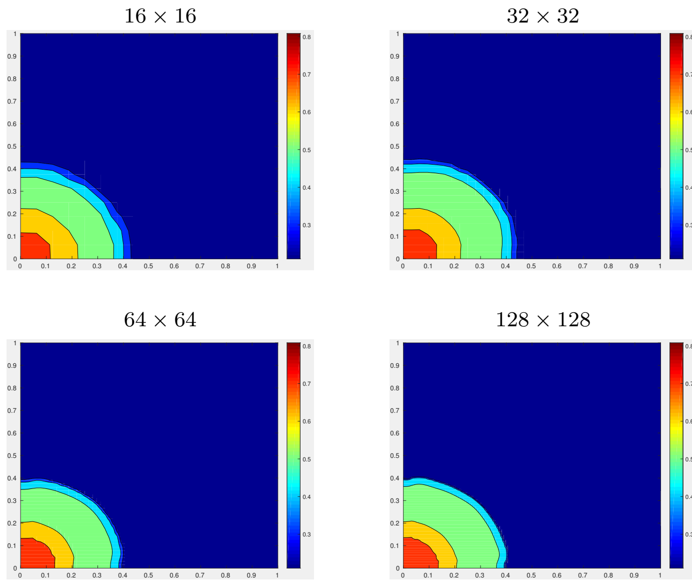

Figure 2: Comparison of saturation contours during a polymer flood in a homogeneous quarter five-spot reservoir with four different spatial resolutions. The contours are plotted at the same time level, $t = 0.5$ to compare the convergence with grid refinement.

References

[1] Prabir Daripa and Sourav Dutta. Modeling and simulation of surfactant polymer flooding using a new hybrid method. Journal of Computational Physics, Under Review 2016.

[2] P. Daripa, J. Glimm, B. Lindquist, M. Maesumi, and O. McBryan. On the simulation of heterogeneous petroleum reservoirs. In Numerical Simulation in Oil Recovery, IMA Vol. Math. Appl. 11, pages 89–103, New York, NY, 1988. Springer.

[3] P. Daripa, J. Glimm, B. Lindquist, and O. McBryan. Polymer floods: A case study of nonlinear wave analysis and of instability control in tertiary oil recovery. SIAM Journal of Applied Mathematics, 48:353–373, 1988.

[4] H. K. Dahle, M. S. Espedal, R. E. Ewing, and O. Svereid. Characteristic adaptive subdomain methods for reservoir flow problems. Numerical Methods for Partial Differential Equations, 6(4):279–309, 1990.

[5] Magne S. Espedal and Richard E. Ewing. Characteristic Petrov-Galerkin subdomain methods for two-phase immiscible flow. Computer Methods in Applied Mechanics and Engineering, 64(1):113 – 135, 1987.

[6] Louis J. Durlofsky. A triangle based mixed finite element-finite volume technique for modeling two phase flow through porous media. Journal of Computational Physics, 105(2):252–266, 1993.

[7] RW Healy and TF Russell. A finite-volume Eulerian-Lagrangian localized adjoint method for solution of the advection-dispersion equation. Water Resources Research, 29(7):2399–2413, 1993.

[8] Peter Bastian. Higher order discontinuous Galerkin methods for flow and transport in porous media. volume 35 of Lecture Notes in Computational Science and Engineering, pages 1–22. Springer Berlin Heidelberg, 2003.

[9] Béatrice Rivière and Mary F. Wheeler. Discontinuous Galerkin methods for flow and transport problems in porous media. Communications in Numerical Methods in Engineering, 18(1):63–68, 2002.

[10] D. Nayagum, G. Schäfer, and R. Mosé. Modelling two-phase incompressible flow in porous media using mixed hybrid and discontinuous finite elements. Computational Geosciences, 8(1):49–73, 2004.

[11] Thomas F Russell and Michael A Celia. An overview of research on Eulerian-Lagrangian localized adjoint methods (ELLAM). Advances in Water Resources, 25(8):1215–1231, 2002.

[12] Hong Wang, Richard E. Ewing, and Thomas F. Russell. Eulerian-Lagrangian localized adjoint methods for convection-diffusion equations and their convergence analysis. IMA Journal of Numerical Analysis, 15(3):405–459, 1995.

[13] J. Douglas Jr., F. Furtado, and F. Pereira. On the numerical simulation of waterflooding of heterogeneous petroleum reservoirs. Computational Geosciences, 1:155–190, 1997.

[14] Hong Wang, Richard E Ewing, Guan Qin, Stephen L Lyons, Mohamed Al-Lawatia, and Shushuang Man. A family of Eulerian-Lagrangian Localized Adjoint Methods for multi-dimensional advection-reaction equations. Journal of Computational Physics, 152(1):120–163, 1999.

[15] Jim Douglas Jr and Thomas F Russell. Numerical methods for convection-dominated diffusion problems based on combining the method of characteristics with finite element or finite difference procedures. SIAM Journal on Numerical Analysis, 19(5):871–885, 1982.

[16] Jim Douglas Jr, Chieh-Sen Huang, and Felipe Pereira. The modified method of characteristics with adjusted advection. Numerische Mathematik, 83(3):353–369, 1999.

[17] Michael A Celia, Thomas F Russell, Ismael Herrera, and Richard E Ewing. An Eulerian-Lagrangian localized adjoint method for the advection-diffusion equation. Advances in Water Resources, 13(4):187–206, 1990.

[18] Todd Arbogast and Mary F Wheeler. A characteristics-mixed finite element method for advection-dominated transport problems. SIAM Journal on Numerical analysis, 32(2):404–424, 1995.

[19] Fuzheng Gao and Yirang Yuan. The characteristic finite volume element method for the nonlinear convection-dominated diffusion problem. Computers & Mathematics with Applications, 56(1):71 – 81, 2008.

[20] Kaixin Wang, Hong Wang, and Mohamed Al-Lawatia. An Eulerian-Lagrangian discontinuous Galerkin method for transient advection-diffusion equations. Numerical Methods for Partial Differential Equations, 23(6):1343–1367, 2007.

[21] Mohammed Shuker Mahmood. Solution of nonlinear convection-diffusion problems by a conservative Galerkin-characteristics method. Numerische Mathematik, 112(4):601–636, 2009.

[22] Jim Douglas Jr, Felipe Pereira, and Li-Ming Yeh. A locally conservative Eulerian-Lagrangian numerical method and its application to nonlinear transport in porous media. Computational Geosciences, 4(1):1–40, 2000.

[23] Hong Wang. An optimal-order error estimate for an ELLAM scheme for two-dimensional linear advection-diffusion equations. SIAM Journal on Numerical Analysis, 37(4):1338–1368, 2000.

[24] Morris Muskat and Milan W. Meres. The flow of heterogeneous fluids through porous media. Journal of Applied Physics, 7(921):346–363, 1936.

[25] R. H. Brooks and A. T. Corey. Properties of porous media affecting fluid flow. Journal of the Irrigation and Drainage Division, 92,(IR2):61–88, 1966.

[26] A. T. Corey. Mechanics of Immiscible Fluids in Porous Media. Water Resources Publications, Littlton, Colorado, 1986.

[27] M. Th. van Genuchten. A closed form equation for predicting the hydraulic conductivity of unsaturated soils. Soil Science Society, 44:892–898, 1980.

[28] J. C. Parker, R. J. Lenhard, and T. Kuppusamy. A parametric model for constitutive properties governing multiphase flow in porous media. Water Resources Research, 23(4):618–624, 1987.

[29] B. Ghanbarian-Alavijeh, A. Liaghat, Guan-Hua Huang, and M. Th. van Genuchten. Estimation of the van genuchten soil water retention properties from soil textural data. Pedosphere, 20(4):456–465, 2010.

[30] S. Hou, W. Wang, and L. Wang. Numerical method for solving matrix coefficient elliptic equation with sharp-edged interfaces. Journal of Computational Physics, 229:7162–7179, 2010.

[31] Z. Li, T. Lin, and X. Wu. New cartesian grid methods for interface problems using the finite element formulation. Numerische Mathematik, 96:61–98, 2003.

[32] James H Bramble. Second order finite difference analogue of the first biharmonic boundary value problem. Numerische Mathematik, 9:236–249, 1966.

[33] Jizhou Li and Béatrice Rivière. Numerical solutions of the incompressible miscible displacement equations in heterogeneous media. Computer Methods in Applied Mechanics and Engineering, 292:107–121, 2014.